ELSEVIER

Journal of Alloys and Compounds 321 (2001) 67–71

Journal of ALLOYS AND COMPOUNDS

www.elsevier.com/locate/jallcom

Micro-mechanical and electrical properties of monolithic aluminum nitride at high temperatures

Jon C. Goldsby*

National Aeronautics and Space Administration, Glenn Research Center, Cleveland, OH 44135, USA

Received 22 September 2000; received in revised form 24 January 2001; accepted 26 January 2001

Abstract

Micromechanical spectroscopy of aluminum nitride reveals it to possess extremely low background internal friction at less than 1×10^{-4} logarithmic decrement (log dec.) from 20 to 1200°C. Two mechanical loss peaks were observed, the first at 350°C approximating a single Debye peak with a peak height of 60×10^{-4} log dec. The second peak was seen at 950°C with a peak height of 20×10^{-4} log dec. and extended from 200 to over 1200°C. These micromechanical observations manifested themselves in the electrical behavior of these materials. Electrical conduction processes were predominately intrinsic. Both mechanical and electrical relaxations appear to be thermally activated processes, with activation energies of 0.78 and 1.32 eV, respectively.

Keywords: Electronic materials; Aluminum nitride high temperature properties; Internal friction high temperature dielectric measurements; Functional ceramics high temperatures

1. Introduction

Aluminum nitride has been shown to have great potential as a high temperature electronic packaging material [1–3]. However in extreme environment applications, low amplitude ($<10^{-6}$ strain) vibrations can be a source of mechanical fatigue and failure. In addition, elevated temperatures encountered during device fabrication and during subsequent operation demand knowledge of the material's temperature-dependent mechanical and electrical response. To obtain this information, resonance frequency and internal friction measurements were performed on aluminum nitride as a function of temperature. The temperature- and frequency-dependent dielectric properties were also measured and compared with the micro-mechanical measurements to elucidate a probable mechanism for the observed behavior.

2. Experimental

Samples of a commercially available aluminum nitride (density 3.27 g/cm^3), with small additions of Y_2O_3 (~1 wt.%) as a consolidation aid, were sectioned into specimens with dimensions 114×9×3 mm. Temperature-dependent elastic and anelastic properties were determined by establishing continuous flexural vibrations in the specimen at its lowest resonance frequency and allowing the vibrations to freely decay after the mechanical excitation was removed. The details of the apparatus are given elsewhere [4]. At a constant frequency (f) the unit for anelastic behavior is the logarithmic decrement ψ and it is calculated as,

$$\psi = \frac{\ln\left(\frac{a_1}{a_2}\right)}{(f)(t_2 - t_1)} \tag{1}$$

where amplitudes a_1 and a_2 are measured at times t_1 and t_2, respectively [11]. The geometry and material-dependent resonance frequency can be calculated from,

$$f = \left(\frac{B}{l^2}\right)\left(\frac{E}{\rho}\right)^{1/2} \tag{2}$$

where B is a combination of geometric and numeric constants, l is the sample length, and E and ρ are the material's elastic modulus and density, respectively. From Eq. (2), a ratio of the resonance frequencies, at a given temperature with respect to the 25°C value, gives a measure of the temperature-dependent elastic response. To obtain the electrical measurements, specimens of aluminum nitride were plated with platinum electrodes. The electric permittivity as a function of temperature and

E-mail address: jon.c.goldsby@grc.nasa.gov (J.C. Goldsby).

0925-8388/01/$ – see front matter
PII: S0925-8388(01)00953-7

frequency was measured in air using a Solatron 1260 impedance analyzer as previously reported [5]. Micrographs of etched and polished samples were recorded using scanning electron microscopy. Energy dispersion spectroscopy (EDS) was used to identify the various major phases of this material.

3. Results and discussion

A typical SEM micrograph is seen in Fig. 1, where three types of features with various amounts of yttrium, alumina, and carbon are clearly revealed. The observed carbon may be only an artifact from the microscope probe analysis. Micrographs of a cut and polished surface reveal grains free of excessive boundary phases. X-ray diffraction also indicates a highly crystalline material. Yttrium-containing compounds appear at grain boundary triple points. In addition, EDS reveals the presence of alumina among the AlN grains.

The mechanical spectrum in Fig. 2 illustrates the anelastic and elastic responses of this material up to 1200°C, at a fundamental vibration of 1464 Hz. This mechanical loss spectrum contains two peaks. The salient features of the first peak include its location at 350°C, with a peak height of 60×10^{-4} log dec. The peak commences at about 200°C and terminates at ~500°C. This energy loss peak closely approximates a Debye peak with a narrow distribution of thermally activated relaxation times. The second mechanical energy loss peak was observed at 950°C, and is designated the high temperature peak. The high temperature peak is a low amplitude, broad peak starting at ~200°C and extending beyond 1200°C. In addition, the mechanical loss spectrum was also obtained

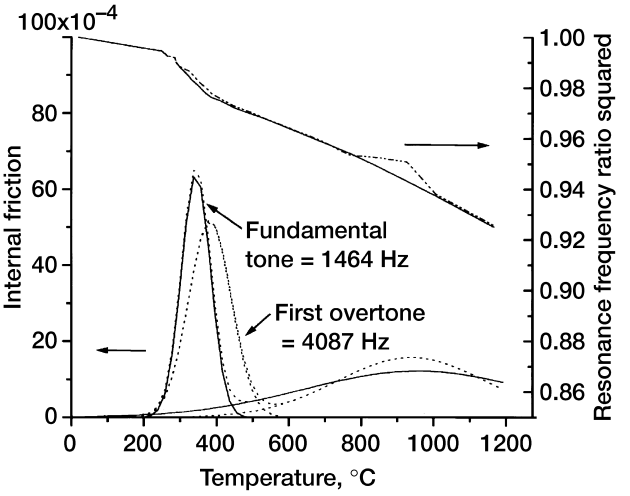

Fig. 2. Temperature dependent elastic and anelastic behavior of aluminum nitride at the fundamental and first overtone flexural vibration frequencies.

at the first overtone to the fundamental frequency, which for this material, vibration mode and geometry was 4087 Hz. This spectrum exhibits the same features as the fundamental tone with the exception of the first overtone peak, which is spectrum-shifted to the right with respect to the temperature. This thermal and mechanical coupling indicates a thermally activated mechanism as the source of the elastic and anelastic dispersion. Noticeably absent is the exponential increase in background internal friction characteristic of the grain boundary sliding observed in silicon nitride [6]. In addition, Fig. 2 also illustrates a decrease or relaxation in the elastic modulus, which occurs at the same temperature as the anelastic relaxation absorption peak at 350°C. The typical elastic response as a function of temperature is shown in the upper curve in Fig.

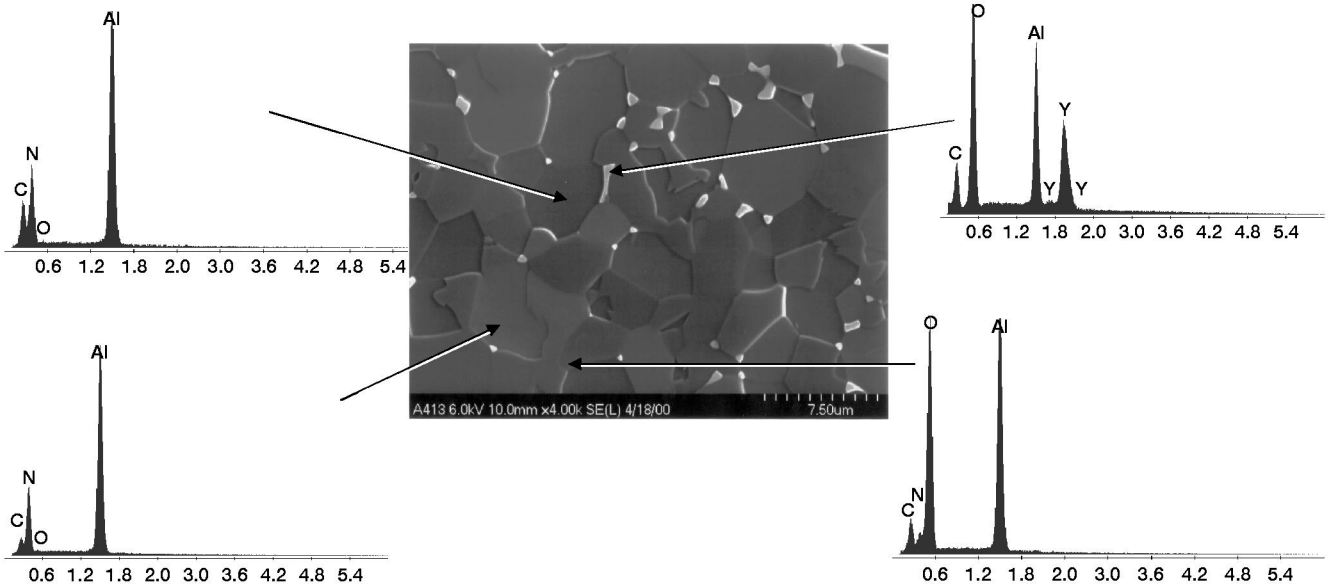

Fig. 1. Micrograph (secondary electron image) of aluminum nitride sample with EDS results illustrating composition.

2. This figure illustrates that the relative stiffness of the material decreases 8% from 25 to 1200°C, which is not unusual for monolithic ceramic materials [4]. In addition features of the elastic response, illustrated in Fig. 2, also shift to higher temperatures when the sample is mechanically excited at its first overtone. This behavior is indicative of a thermally activated mechanism. Because such a low level of internal friction exists around the peaks and the corresponding temperature-dependent elasticity remains relatively constant, no evidence of grain boundary sliding-induced micro-creep is evident, under the conditions of the micro-strains imposed on the aluminum nitride samples in this investigation.

Given the reported piezoelectric nature of bulk and thin film AlN [7], temperature-dependent dielectric measurements were performed to determine if these micromechanical observations manifested themselves in the electrical properties of this material. The complex electric modulus (M) formalism was used to characterize the material's temperature-dependent dielectric properties [8,9]. The complex electric modulus is the reciprocal of the complex permittivity ε. The relationship between the permittivity and the electric modulus is given in Eq. (3)

$$M = \frac{1}{\varepsilon} = \frac{\varepsilon_{\text{Real}}}{\varepsilon^2_{\text{Real}} + \varepsilon^2_{\text{Imaginary}}} + j\frac{\varepsilon_{\text{Imaginary}}}{\varepsilon^2_{\text{Real}} + \varepsilon^2_{\text{Imaginary}}}. \quad (3)$$

The complex electric modulus plot gives a single arc, which is representative of the bulk properties of the material (Fig. 3). From these data, the magnitude of the imposed alternating electric field and sample dimensions, the direct current resistivity was determined to be 10^8 Ω/m. Therefore this AlN sample, with predominately covalent bonding, behaves like an insulator and hence contains minimal concentrations of those agents, which could function as extrinsic charge carrying dopants.

Results shown in Fig. 4 illustrate a dispersion of the real part of the electric modulus. The midpoints of these dispersion curves occur at 10, 20, 30, and 70 kHz for these temperatures 466, 490, 515, and 550°C, respectively. The peaks in Fig. 5a and b appear thermally activated and are located near the temperature of the mechanical internal

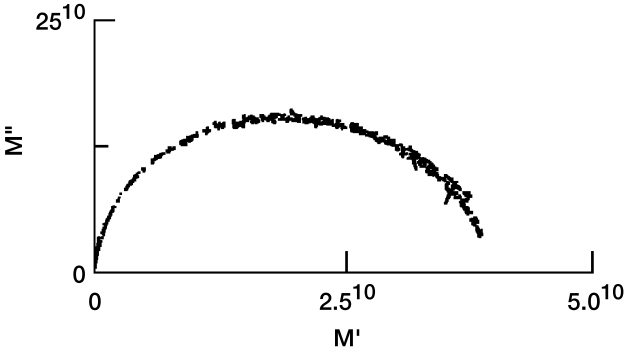

Fig. 3. Complex electric modulus plot of aluminum nitride.

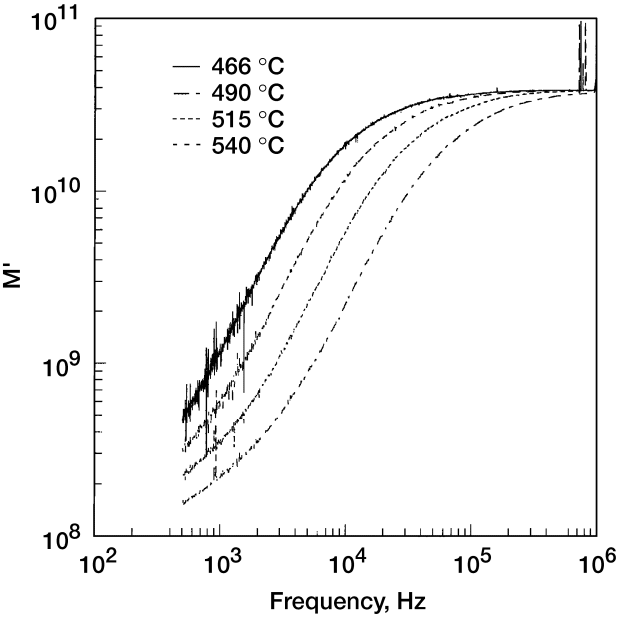

Fig. 4. Frequency and temperature dependent real part of the electric modulus.

friction peak found at 400°C and 4087 Hz. Each peak extends over three decades of frequency, indicating a wide range of relaxation times due to the non-degenerate reorientation of elastic strain energy states of the relaxing entities. At higher temperatures (560 to 734°C), the complex component of the electric modulus becomes narrower and higher as compared to the lower temperature results (Fig. 5a and b). In addition it is at these temperatures that the two mechanical loss peaks overlap in Fig. 2. The smaller peak at 560°C in Fig. 5b appears to be a continuation of the low temperature peaks seen in Fig. 5a. The higher and narrower absorption curves in Fig. 5b, suggest a different source of origin, possibly one that is related to the high temperature loss peak in Fig. 2.

Both the mechanical and electrical energy absorption peaks can be treated as thermally activated Arrhenius processes to obtain their respective activation energies. The energy equation is classically expressed as

$$f(T) = f_0 e^{(-Q/kT)} \quad (4)$$

where $f(T)$ is the temperature-dependent resonance frequency, f_0 is the characteristic frequency of the relaxation phenomenon, k and T are the Boltzmann constant and absolute temperature, respectively, and Q represents the activation energy. A plot of the peak frequency as a function of reciprocal temperature is given in Fig. 6. From the slope of these lines the activation energy was found to be 0.78 eV for the $T = 350$°C mechanical anelastic peak. Activation energies derived from the electric modulus were 1.32 and 1.18 eV for the low temperature and high temperature peaks, respectively. Nakayama et al. [10] have observed the loss tangent as a function of grain size, and

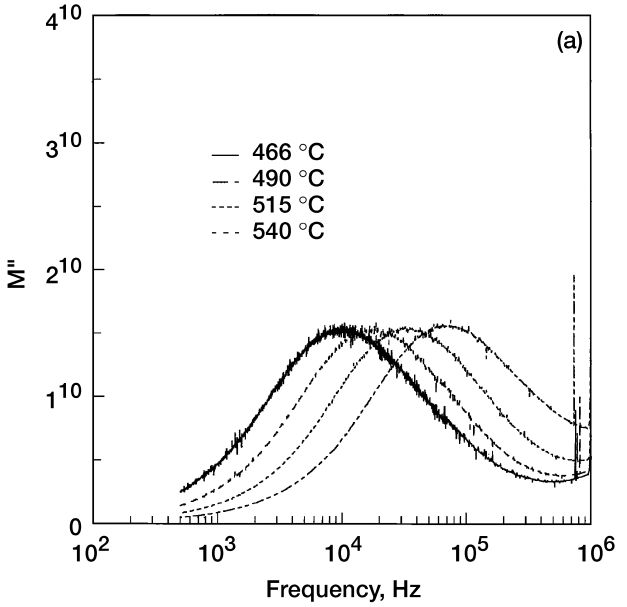

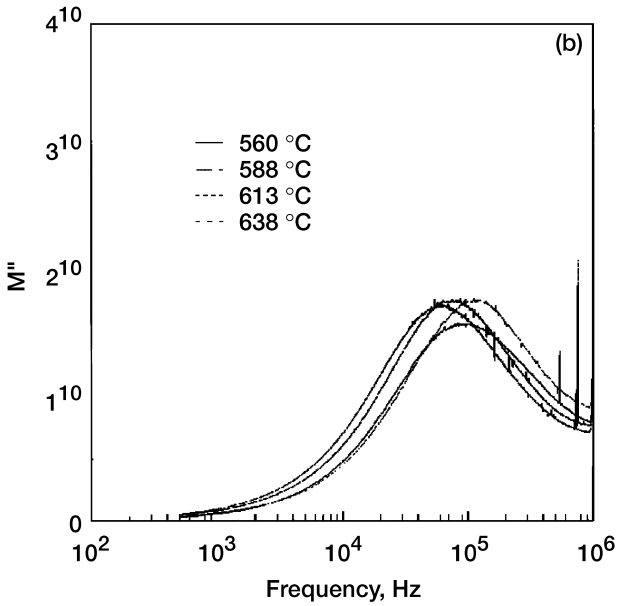

Fig. 5. Frequency and temperature dependence of the imaginary part of the electric modulus (a) from 466°C to 540°C and (b) from 560°C to 638°C.

attributed the energy absorption peak to the piezoelectric effect in AlN crystal grains at 830 MHz and 30°C. Hence in this study the magnitude of the thermal activation energies, temperatures, frequencies and height of the mechanical absorption peak indicate that the piezoelectric effect is not the source of the observed mechanical or electrical dispersion in the loss factors. The results of this investigation are more indicative of point defects or a cluster of point defects as the likely cause of the electrical and mechanical relaxation [10,11].

Slack et al. [12] have identified oxygen as a major impurity in aluminum nitride. One possible source of

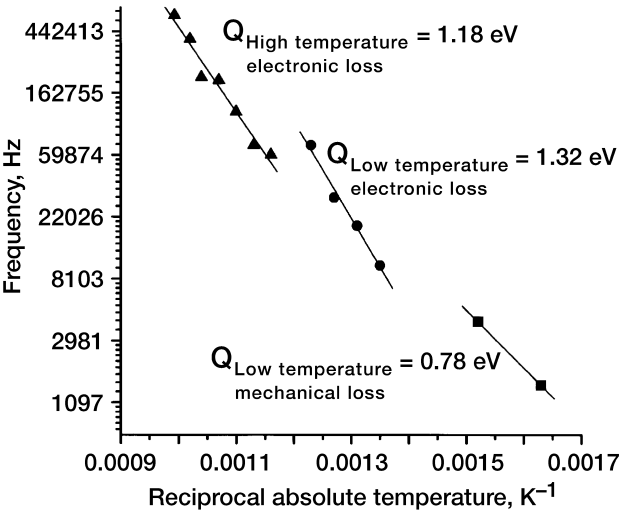

Fig. 6. Determination of activation energies for mechanical and electronic loss processes in aluminum nitride.

oxygen clearly would be the consolidation additives, examples of which are Al_2O_3 and Y_2O_3 as seen in Fig. 1. Eq. (5) is the proposed mechanism for the incorporation of M_2O_3, where M is a metal in the (+3) state, into AlN expressed in Kröger–Vink notation. In this scenario lattice misfit strain occurs due to the smaller ionic radii of the incorporated oxygen, as compared with the nitrogen ion of the host crystal. In addition, to compensate for the difference in valance, charged (+2) vacancies on the aluminum sites are created

$$M_2O_3 \overset{AlN}{\leftrightarrow} 2M_{Al}^{\bullet} + 3O_N^{\bullet} + V_{Al}''' \quad (5)$$

The resultant physical entity, which is described by Eq. (5), is a charged defect cluster within the AlN crystal lattice. This defect or electro-elastic dipole would respond to both external mechanical and electrical alternating fields. The probable cause for the different magnitudes between the mechanical and electrical activation energies at the lower temperatures may be due to the difference in the elastic strain energy barrier to reorientation. The externally applied alternating mechanical stress field may provide sufficient elastic strain energy to reduce the reorientation barrier and hence lower the activation energy needed for the defect's reorientation. A similar effect may be functioning at the higher temperature electric relaxation. At higher temperatures a more isotropic stress state may exist due to thermal expansion of the crystal lattice and thereby lowering the activation energy for defect reorientation.

4. Conclusions

Temperature-dependent elastic, anelastic, and electrical properties of AlN were characterized by micro-mechanical

and dielectric measurements. Intrinsic damping in aluminum nitride was below that needed to suppress vibrations at temperatures below 1200°C in vacuum. In addition, alternating stress and electrical fields induced dipole reorientation of vacancy defects. The elastic modulus only decreased by 8% under the conditions of this investigation (20 to 1200°C), and hence aluminum nitride has the potential of retaining stiffness and dimensional tolerances at elevated temperatures.

References

[1] A.F. Belyanin, L.L. Bouilov, V.V. Zhirnov, A.I. Kamenev, K.A. Kovalskij, B.V. Spitsyn, Application of aluminum nitride films for electronic devices, Diamond Relat. Mater. 8 (2–5) (1999) 369–372.
[2] S.P. McGeoch, F. Placido, Z. Gou, C.J.H. Wort, J.A. Savage, Coatings for the protection of diamond in high-temperature environments, Diamond Relat. Mater. 8 (2–5) (1999) 916–919.
[3] J.H. Harris, Sintered aluminum nitride ceramics for high-power electronic applications, JOM 50 (6) (1998) 56–60.
[4] J.C. Goldsby, Temperature-dependent elastic and anelastic behavior of silicon-based fiber reinforced silicon carbide ceramic matrix composites, Mater. Sci. Eng. A A279 (2000) 266–274.
[5] P.W. Angel, M.R. De Guire, A.R. Cooper, Electrical conductivity, relaxation and the glass transition: a new look at a familiar phenomenon, J. Non-Cryst. Solids 203 (1996) 286–292.
[6] R. Raj, M.F. Ashby, On grain boundary sliding and diffusion creep, Metall. Trans. 2 (1971) 1113–1127.
[7] A. Nakayanna, S. Nambu, M. Inagaki, M. Miyauchi, N. Itoh, Dielectric dispersion of polycrystalline aluminum nitride at microwave frequencies, J. Am. Ceram. Soc. 79 (6) (1996) 1453–1456.
[8] I.M. Hodge, M.D. Ingram, A.R. West, Impedance and modulus spectroscopy of polycrystalline solid electrolytes, J. Electroanal. Chem. Interfacial Electrochem. 74 (1976) 125–143.
[9] I.M. Hodge, M.D. Ingram, A.R. West, A new method for analyzing the a.c. behaviour of polycrystalline electrolytes, Electroanal. Chem. Interfacial Electrochem. 58 (1975) 429–432.
[10] L. Murawski, R.J. Barczynski, D. Samatowicz, O. Gzowski, Correlation between mechanical and electrical losses in transition metal oxide glasses, J. Alloys Comp. 211–212 (1994) 344–348.
[11] A.S. Nowick, B.S. Berry, Anelastic Relaxation in Crystalline Solids, Academic Press, New York, 1972.
[12] G.A. Slack, R.A. Tanzilli, R.O. Pohl, J.W. Vandersande, The intrinsic thermal conductivity of AlN, J. Phys. Chem. Solids 48 (78) (1987) 641–647.